https://doi.org/10.5194/egusphere-2026-3086
Preprint. Discussion started: 12 June 2026

Extending terrestrial water storage anomalies beyond the GRACE era using tree rings

Lucas E. B. Hoeltgebaum[1], Grant L. Harley[1], Meng Zhao[1]

[1]Department of Earth and Spatial Sciences, University of Idaho, Moscow, ID 83843, USA

Correspondence to: Meng Zhao (mengz@uidaho.edu)

Abstract. Satellite observations from NASA's Gravity Recovery and Climate Experiment (GRACE) and GRACE Follow-On have transformed monitoring of terrestrial water storage (TWS) anomalies, but their short record (2002–present) limits characterization of long-term variability and extremes. Here, we evaluate whether tree-ring width indices (RWI) can be used to extend TWS variability across western North America. Using 144 chronologies, we find predominantly positive correlations between RWI and GRACE-observed TWS anomalies, with mean annual correlations of r = 0.25 (IQR: 0.07–0.50) and the strongest relationships during summer (mean r = 0.27; 37% of sites significant at $p < 0.1$). Correlation strength is highest in moisture-limited environments and among Pinus species. In the Upper Colorado River Basin, a two-site composite model explains 69% of the variance in GRACE-observed summer TWS anomalies (r = 0.83) and enables reconstruction back to 1567 CE. The reconstruction exhibits a standard deviation of 29.9 mm and a peak-to-trough range of 167.6 mm, and agrees well with other hydroclimatic records, including reconstructed Palmer Drought Severity Index over 1567-2000 (r = 0.79) and climate-data-driven TWS estimates over 1901-2000 (r = 0.73). Using climate-data-driven TWS estimates as a longer reference record, moving-window analyses show that calibration stability improves rapidly from 10-year to approximately 25–30-year windows, after which additional years yield more gradual gains. Together, these results suggest that the now nearly 25-year GRACE and GRACE Follow-On record is approaching the duration needed for more stable tree-ring–TWS calibration, and that targeted extension of moisture-sensitive chronology networks through the satellite era may provide a robust pathway for reconstructing multi-century TWS variability in western North America and other similar regions.

1 Introduction

The Gravity Recovery and Climate Experiment (GRACE), launched in 2002, and its successor mission, GRACE Follow-On, hereafter collectively referred to as GRACE, measure monthly changes in Earth's gravity field, which at monthly timescales are driven largely by the redistribution of water (Tapley et al., 2004). These observations enable monitoring of changes in total terrestrial water storage (TWS), including groundwater, soil moisture, surface waters, snow, and ice. This capacity has transformed monitoring hydrological extremes and characterize changes in water storage change over the satellite era (Chandanpurkar et al., 2025; Reager et al., 2014; Rodell et al., 2018; Rodell & Li, 2023; Thomas et al., 2014; M. Zhao et al.,

https://doi.org/10.5194/egusphere-2026-3086
Preprint. Discussion started: 12 June 2026

2017a). However, the relatively short duration of GRACE record limits the extent to which recent droughts, pluvials, and TWS long term trends can be interpreted in a broader historical context. As a result, it remains difficult to determine whether events observed during the satellite era are unusual relative to earlier decades or to robustly attribute long-term TWS changes to climate variability, climate change, or human influence (Buzzanga et al., 2025; Chandanpurkar et al., 2025; Rodell et al., 2018; Rodell & Li, 2023). Addressing these questions requires TWS records extending well beyond the satellite era. Several studies have reconstructed TWS anomalies back to approximately 1900 using climate data combined with statistical or machine learning approaches (Humphrey & Gudmundsson, 2019; Li et al., 2020, 2021; Yin et al., 2023; Hacker et al., 2026), however, these reconstructions still fall short of providing the multi-century context needed to fully evaluate TWS changes over the timescales relevant to human-driven climate change.

Tree rings are well established as annual-resolution archives that extend hydroclimatic variability back multiple centuries (Speer, 2010), making them promising proxies for reconstructing TWS anomalies over comparable timescales. In water-limited regions, tree-ring width reflects interannual growth variations that are strongly constrained by moisture availability (Cook et al., 2010; Meko & Woodhouse, 2010; Williams et al., 2022; Yang et al., 2014). Because trees can access water from both saturated and unsaturated zones, including snowmelt, surface water, root-zone soil moisture, groundwater, and moisture stored in weathered bedrock (McCormick et al., 2021; Stocker et al., 2023; Woodhouse, 2003; M. Zhao et al., 2025), tree growth captures integrated surface and subsurface water availability rather than only immediate precipitation inputs (Maxwell et al., 2022). This integrative sensitivity suggests that tree-ring variability may well align with TWS variability. Yet, despite this conceptual link, large-scale, multi-century reconstructions of TWS remain largely unexplored. To our knowledge, only one prior study has examined this relationship: Creutzfeldt et al. (2015) demonstrated the feasibility of reconstructing TWS anomalies from tree-ring sites using local gravimeter observations, though at limited spatial scales.

Here, we assess the potential for tree-ring chronologies to track large-scale TWS variability across western North America. We focus on this region because it encompasses extensive water-limited ecosystems, exhibits strong hydroclimatic variability, and benefits from a substantial archive of previously collected moisture-sensitive tree-ring records. Specifically, we ask whether tree-ring chronologies are correlated with GRACE TWS anomalies, which seasonal window of TWS is most strongly associated with tree-ring variability, what factors govern tree-ring sensitivity to TWS, and whether the short GRACE record contains sufficient information to support a meaningful reconstruction. Using 144 tree-ring chronologies selected from across western North America, we evaluate the strength and controls of tree-ring–TWS relationships and demonstrate that moisture-sensitive tree rings capture a coherent TWS signal that is strongest during the summer growing season, enabling basin-scale reconstruction of water storage variability beyond the satellite era, as illustrated for the Upper Colorado River Basin back to the mid-1500s CE.

https://doi.org/10.5194/egusphere-2026-3086
Preprint. Discussion started: 12 June 2026

2 Data and Methods

2.1 Tree-ring and GRACE datasets

We used standardized tree-ring width index (RWI) chronologies of tree-ring compiled by Williams et al. (2020a, 2020b) for western North America, largely derived from the International Tree-Ring Databank. Each site chronology is based on multiple (typically ≥10) tree cores and constructed from raw ring-width measurements. To isolate climate signals, non-climatic biological growth trends were removed using conservative, signal-free detrending methods designed to preserve low-frequency variability (Fritts, 2012; Melvin & Briffa, 2008). Specifically, age-dependent spline functions were applied to each series, following power transformation, and indices were calculated as residuals from the fitted growth curve (Cook & Peters, 1997; Fritts et al., 1969; Melvin et al., 2007). Site-level chronologies were then generated using a bi-weight robust mean across individual series (Hoaglin et al., 2000). To address non-climatic variance changes associated with sample depth and tree age, variance stabilization was applied to the final chronologies using an age-based spline (Meko et al., 1993).

We obtained monthly GRACE TWS anomalies from the JPL RL06 mascon product for 2002–2016. The JPL product estimates monthly gravity variations over equal-area 3° × 3° mass concentration blocks, or mascons. We used this solution because it exhibits relatively low spatial correlation among neighboring mascons and is well suited for resolving localized mass-change signals (Watkins et al., 2015; Wiese et al., 2016). Missing monthly values within the study period were linearly interpolated from the nearest available valid months (Rodell et al., 2018).

Most tree-ring chronologies in the network terminate around 2010, and none of the chronologies used here extend beyond 2017. We therefore restricted the satellite comparison to the GRACE period (2002-2017) rather than including GRACE Follow-On (2018-present). To ensure adequate temporal overlap, we retained only chronologies with at least 10 years of common coverage during the GRACE period, yielding 144 sites across western North America. Details on tree-ring site selection and site naming based on available metadata are provided in Appendix A, and Table A1 lists the scientific and common names of the tree species included in the study, along with the species codes used in the analyses.

2.2 TWS-RWI correlation analysis

To evaluate whether tree-ring variability reflects large-scale water storage, we calculated Pearson correlation coefficients between annual RWI and GRACE-derived TWS anomalies at each site. Although individual tree-ring sites and GRACE mascons represent different spatial scales, tree-ring chronologies are commonly used to reconstruct gridded hydroclimatic fields and basin-scale variables using search radii comparable to or larger than GRACE mascons (e.g., 450–700 km; (Cook et al., 2004; Singh Chuphal et al., 2025)). We therefore paired each chronology with the GRACE mascon in which it is located. Monthly TWS anomalies were aggregated to annual means (calendar year, from January to December) and seasonal

https://doi.org/10.5194/egusphere-2026-3086
Preprint. Discussion started: 12 June 2026

means for spring (MAM), summer (JJA), fall (SON), and winter (DJF). Because water-year averaging may better capture hydrologic storage carryover in western U.S. basins, we also repeated the annual analysis using water-year mean TWS (from October to September). These annual and seasonal TWS metrics were then paired with annual RWI values for correlation analysis. Statistical significance was assessed using a two-sided test with a threshold of $p < 0.1$, reflecting the limited overlap period between GRACE observations and tree-ring records.

2.3 Environmental controls on TWS-RWI relationships

To identify factors governing spatial variability in TWS–RWI correlations, we examined relationships between correlation strength and vegetation type, climate, and topography. Vegetation was characterized using species or genus information associated with each chronology. Climate variables included mean annual precipitation and mean annual 2-m air temperature from CONUS404, a 4-km resolution hydroclimate dataset (Rasmussen et al., 2023). Elevation was taken from the site metadata when available; missing values were filled using the 30-m Shuttle Radar Topography Mission digital elevation model (NASA, 2013).

2.4 Tree-ring–based reconstruction of basin-scale TWS anomalies

We developed a statistical framework to reconstruct basin-scale TWS anomalies using tree-ring chronologies, demonstrated for the Upper Colorado River Basin. We selected this basin because, among western North American basins, it provides a favorable combination of GRACE-era chronology overlap, spatially distributed sites, and strong TWS–RWI coupling, making it suitable for testing basin-scale reconstruction. Because tree-ring width primarily integrates growing-season conditions, we focused the reconstruction on summer TWS anomalies. Chronology sites within the basin were first screened based on their correlations with basin-averaged summer TWS anomalies during the GRACE period. Individual RWI series were standardized as z-scores to account for differences in mean and variance among sites. We evaluated reconstruction approaches commonly used in dendroclimatology, including multiple linear regression with predictor selection based on Akaike information criterion (AIC) and dimensionality reduction using principal component analysis (Littell et al., 2016). However, with only slightly more than a decade of GRACE overlap observations, these approaches are sensitive to sampling noise and prone to overfitting. In particular, AIC-based model selection indicated that including additional chronologies or principal component beyond a single predictor did not yield sufficient improvement in fit to justify the increased model complexity, suggesting that the available calibration data do not support multi-predictor models (Appendix B). Although AIC-based selection favors a single predictor under the short calibration period, we constructed a composite chronology to improve spatial representativeness and reduce sensitivity to site-specific noise. Specifically, we averaged the standardized RWI series across selected sites. This approach provides a parsimonious form of dimensionality reduction, reduces model complexity, limits overfitting, and emphasizes variability that is coherent across chronologies while suppressing site- and

https://doi.org/10.5194/egusphere-2026-3086
Preprint. Discussion started: 12 June 2026

species-specific noise. We then fitted simple linear regression models relating the composite RWI predictor to GRACE-derived summer TWS anomalies over the satellite era. To identify an optimal chronology subset, sites were added progressively in order of decreasing correlation strength with TWS, and model performance was evaluated at each step. The final model was selected as the chronology combination that achieved the highest correlation with GRACE-derived TWS anomalies during their common period. The calibrated relationship was then applied to the full length of the selected chronologies to reconstruct historical summer TWS anomalies.

Basin-scale GRACE TWS anomalies were estimated using an area-weighted aggregation of intersecting mascons (Y. Zhao et al., 2025). For each mascon overlapping the Upper Colorado River Basin, we calculated its fractional contribution to the total basin area and used these fractions as weights when averaging the corresponding mascon-level TWS anomaly time series.

To estimate uncertainty in the reconstruction of TWS anomalies, we considered two primary error sources: GRACE measurement uncertainty and regression model error. To quantify the influence of GRACE measurement uncertainty, we conducted a Monte Carlo simulation by adding random noise to the monthly GRACE TWS anomalies, with zero mean and standard deviation equal to the reported monthly GRACE measurement error. This procedure generated 1,000 pseudo-TWS time series, each of which was processed through the same reconstruction process. The standard deviation of the resulting 1,000 reconstructions was used as a proxy for uncertainty associated with GRACE measurement error. Regression model error was estimated as the root-mean-square error (RMSE) between reconstructed and GRACE-derived TWS anomalies during their common period. Total reconstruction uncertainty was then estimated by combining the GRACE-related uncertainty and regression error in quadrature (M. Zhao et al., 2021).

To evaluate the reconstructed TWS anomalies, we compared them with tree-ring-based Palmer Drought Severity Index (PDSI) reconstructions (Steiger et al., 2018). Although both products use tree-ring information, they are not interchangeable because their site networks are optimized to represent different hydroclimatic processes (Fig. C2). PDSI is designed to represent atmospheric dryness and surface soil moisture drought (M. Zhao et al., 2017b), whereas our reconstruction targets basin-scale terrestrial water storage. We also compared the reconstructed TWS anomalies with 1901–2014 TWS estimates derived from instrumental climate data calibrated against GRACE-derived TWS (Humphrey & Gudmundsson, 2019), hereafter referred to as climate-data-driven TWS estimates, to provide an evaluation independent of tree-ring data. Because the climate-data-driven TWS estimates begin in 1901, evaluation of the pre-1901 reconstruction relies on comparison with the PDSI reconstruction.

https://doi.org/10.5194/egusphere-2026-3086
Preprint. Discussion started: 12 June 2026

3 Results

3.1 TWS-RWI correlation patterns

Positive correlations between calendar year annual mean TWS and RWI dominate across sites, indicating that tree-ring width captures interannual variability in TWS across much of the western United States (Fig. 1a). This pattern is robust to the definition of the annual averaging period: using water-year rather than calendar-year mean TWS produces similar correlations and does not systematically improve agreement with RWI (Fig. C3). A smaller number of negative correlations are found, mainly at higher latitudes and elevations in the Rockies and Cascades. Across the 144 sites, the mean correlation between annual mean TWS and RWI is 0.25, with an interquartile range (IQR) of 0.07 to 0.50. Seasonal TWS–RWI correlations (Figs. 1b-e) are broadly consistent with this annual pattern, remaining predominantly positive and suggesting that tree growth reflects TWS variability across multiple seasons, with the strongest associations in summer. Mean correlations are 0.22 for spring (MAM; IQR: 0.00 to 0.48), 0.27 for summer (JJA; IQR: 0.02 to 0.55), 0.18 for fall (SON; IQR: −0.03 to 0.44), and 0.14 for winter (DJF; IQR: −0.15 to 0.43). Considering only statistically significant correlations ($p < 0.1$) yields the same overall pattern: 30% of sites are significant for annual mean TWS, summer has the largest fraction of significant sites (37%), and winter the smallest (19%) (Fig. 1f).

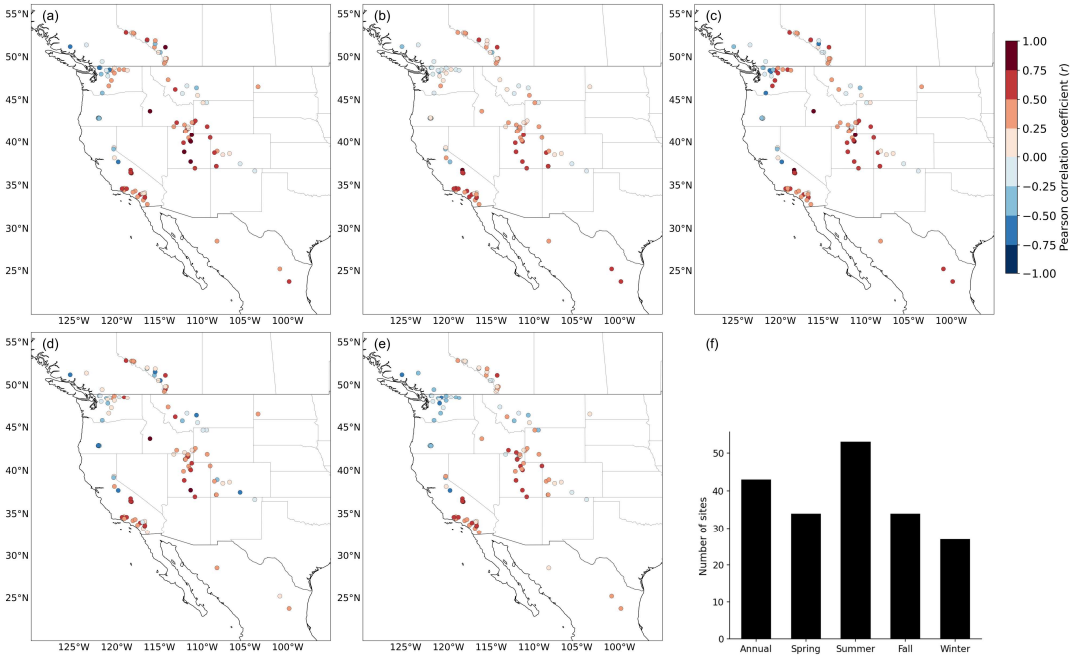

https://doi.org/10.5194/egusphere-2026-3086
Preprint. Discussion started: 12 June 2026

Figure 1: Pearson correlation coefficient between RWI and (a) annual mean TWS (calendar year). (b)-(e): same for spring TWS (MAM), summer (JJA), fall (SON), and winter (DJF). (f) Number of sites with significant correlations ($p < 0.1$) between TWS and RWI for all seasons.

3.2 Controls on TWS-RWI correlations

To better understand where tree-ring records reliably capture TWS variability, we focus primarily on summer TWS, which exhibits the overall strongest relationship with annual RWI (Sect. 3.1), and examine the influence of vegetation type, climate, and topography to inform site selection for TWS reconstruction. Vegetation type emerges as the primary factor associated with variability in TWS–RWI correlations, indicating strong differences in the ability of different taxa to represent large-scale water storage variability. In particular, sites associated with the Pinus genus exhibit the highest correlations with TWS. Because Pinus is the most widely represented genus in our dataset and shows substantial within-genus variability, we further separate *Pinus* records by subsection to evaluate whether this genus-level pattern is driven by particular taxa. Species within each *Pinus* subsection are shown in Table A1 in the Supplement. Subsections such as *P. balfouriana*, *P. ponderosa*, *P. coulteri*, and *P. cembroides* show consistently strong positive correlations, whereas *P. strobus* exhibits notably weaker relationships (Fig. 2a). For other genera, species-level sample sizes are too limited to support robust within-genus comparisons, so they are retained at the genus level. Unlike *Pinus*, a smaller subset of vegetation types, particularly the *Tsuga* genus, is associated with predominantly negative correlations. These sites are primarily located in the cooler, high-precipitation environments of the Pacific Northwest (Fig. C4). In such regions, tree growth is often energy-limited and strongly influenced by temperature and snowpack dynamics (Gedalof & Smith, 2001; Littell et al., 2023), reducing the extent to which tree-ring width tracks variations in large-scale water storage. As a result, increases in TWS do not necessarily correspond to enhanced growth, leading to weak or negative correlations.

To examine environmental controls on TWS-RWI relationships, sites were grouped into approximately equal-sample bins for each environmental variable, including mean annual precipitation, mean annual temperature, and elevation. Equal-sample bins were used rather than evenly spaced intervals because the number of sites is limited and unevenly distributed across climate and topographic gradients. This strategy avoids overinterpreting sparsely sampled ranges while preserving broad environmental patterns. Correlation strength tends to decline with increasing mean annual precipitation, indicating that tree-ring records more reliably reflect TWS variability in relatively dry environments (Fig. 2b). In contrast, we find no clear relationship between TWS–RWI correlations and either elevation or mean annual temperature across the sampled sites (Figs. 2c-d). However, because site selection was constrained by overlap with the GRACE record, the sampled chronologies do not span the full topographic and climatic range of western North America. The absence of significant relationships with elevation or mean annual temperature should therefore not be interpreted as evidence that these variables are unimportant more broadly. Although this analysis focuses on summer TWS–RWI correlations, these controls are broadly consistent

https://doi.org/10.5194/egusphere-2026-3086
Preprint. Discussion started: 12 June 2026

across annual and other seasonal correlations (Figs. C5-C8), reinforcing their relevance for identifying sites suitable for TWS reconstruction.

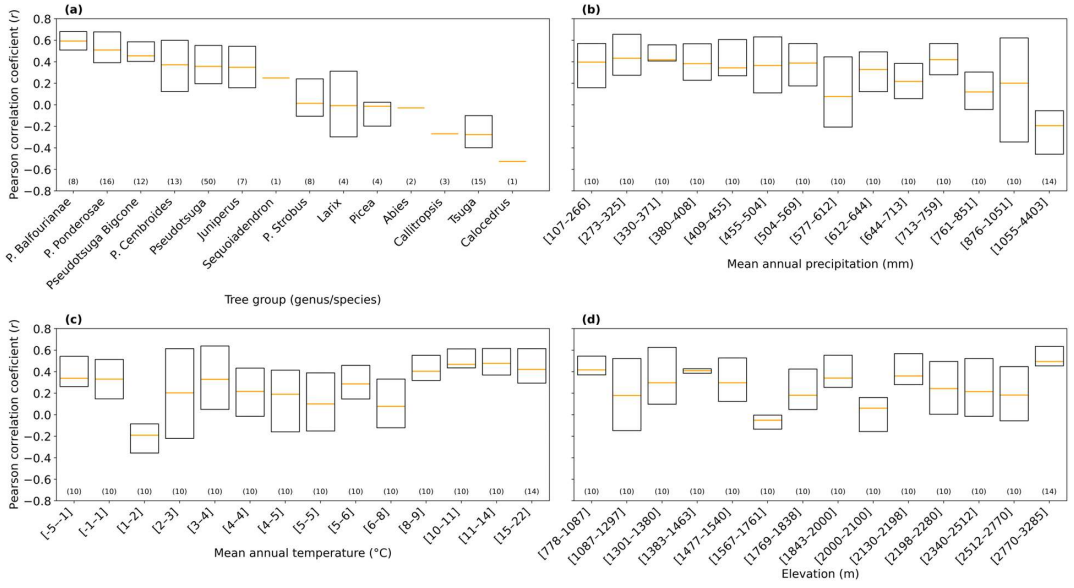

Figure 2: Pearson correlation coefficient distribution between summer GRACE TWS and RWI across (a) tree group (genus/subsections), (b) mean annual precipitation, (c) mean annual temperature, and (d) elevation. Boxes show the interquartile range, orange lines indicate the mean, and numbers above each bin indicate the number of sites.

3.3 A case study of TWS reconstruction in the Upper Colorado River Basin

To demonstrate the feasibility of reconstructing basin-scale TWS anomalies from tree-ring records, we conducted a case study in the Upper Colorado River Basin. Unlike many dendroclimatic reconstructions, this case study is constrained by the short overlap between available chronologies and GRACE observations. We therefore treat the reconstruction as a proof-of-concept rather than a definitive reconstruction product. Following the approach described in Sect. 2.4, candidate chronologies were screened against basin-averaged summer GRACE TWS anomalies, standardized as z-scores, and averaged into a composite predictor to reduce model complexity and limit overfitting under the short calibration period.

The highest reconstruction skill was obtained using a two-site composite based on the UNAWEP and USCHUL chronologies (Fig. 3a), which explains more than two-thirds of the variance in GRACE-observed summer TWS anomalies during the 12-year calibration period (R2 = 0.69; Fig. 3b). Leave-one-out cross validation produced a reduction of error

https://doi.org/10.5194/egusphere-2026-3086
Preprint. Discussion started: 12 June 2026

statistic of 0.31, indicating positive predictive skill despite the limited calibration sample. The two sites share a common record spanning 1567–2013 CE, enabling a multi-century reconstruction of summer TWS anomalies.

The reconstructed TWS anomalies exhibit substantial interannual variability, with a standard deviation of 29.89 mm and a total range of 167.57 mm between maximum and minimum values (Fig. 3c). The mean total reconstruction error is 24.65 mm, indicating that the reconstruction captures a meaningful hydrologic signal despite the short satellite-era calibration period (Fig. C9). Consistent with this, the tree-ring–based reconstruction of TWS anomalies shows strong agreement with complementary hydroclimatic reconstructions. Reconstructed TWS anomalies are highly correlated with tree-ring–based PDSI ($r = 0.79$ for 1567–2000) and with TWS anomaly reconstructions derived from instrumental climate data ($r = 0.73$ for 1901–2000). The reconstructed TWS anomalies and PDSI share similar multi-decadal variability, although differences in timing are evident for some events, such as the 1625–1650 drought, during which PDSI leads TWS anomalies during both intensification and recovery (Fig. 3c). Agreement with climate-data-driven TWS estimates is strongest during 1950–2000, whereas larger differences occur during 1901–1950, when the tree-ring–based reconstruction remains more consistent with PDSI, especially in indicating the extreme wet conditions of the 1910s. Overall, these comparisons show that the reconstructed TWS anomalies capture large-scale hydroclimatic variability, agree well with alternative TWS reconstructions, and provide information complementary to PDSI, supporting the use of tree-ring records to extend basin-scale TWS variability beyond the satellite era.

https://doi.org/10.5194/egusphere-2026-3086
Preprint. Discussion started: 12 June 2026

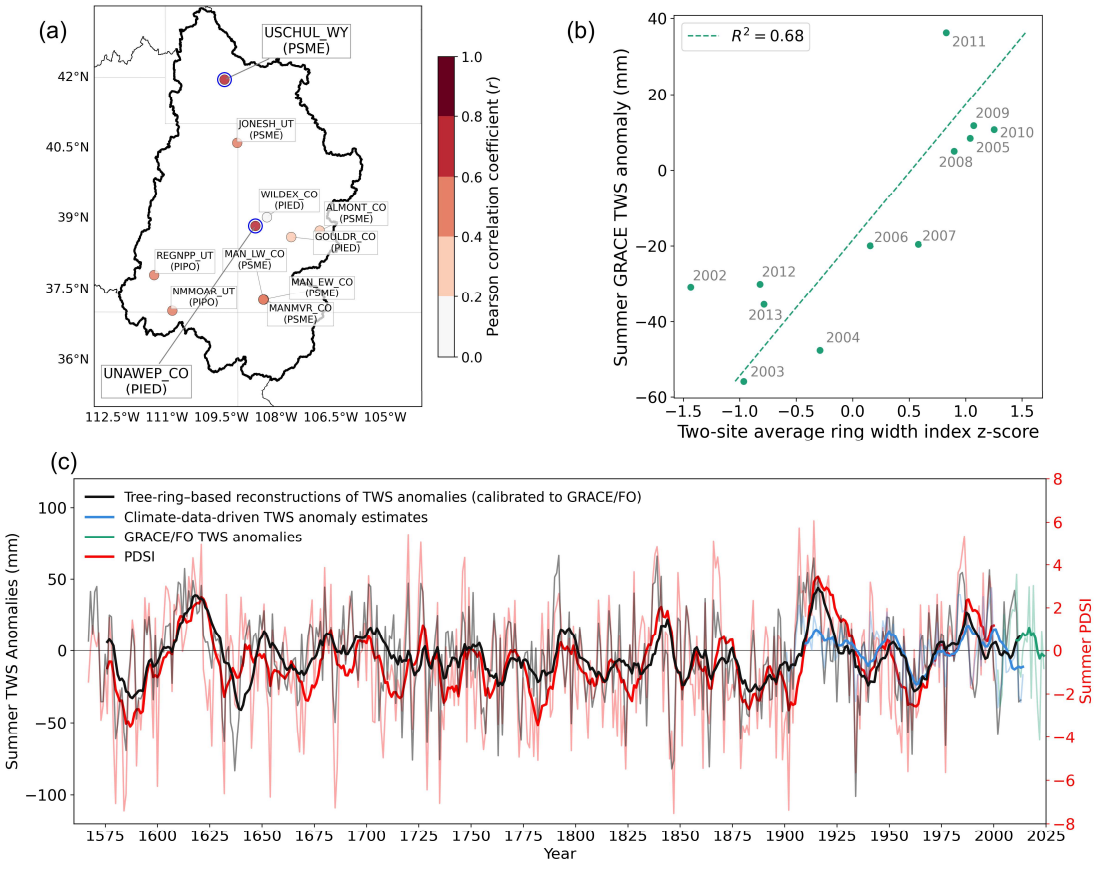

245 **Figure 3:** Two moisture-sensitive tree-ring chronologies capture basin-scale TWS variability in the Upper Colorado River Basin. (a) Tree-ring chronology sites, with the two chronologies used for reconstruction highlighted by blue circles; colors indicate correlations with summer basin-scale GRACE-derived TWS anomalies. (b) Relationship between summer GRACE TWS anomalies and the mean z-score tree-ring width index from sites USCHUL_WY and UNAWEP_CO. (c) Basin-wide tree-ring-based summer TWS anomaly reconstruction compared with climate-data-driven TWS estimates (Humphrey & Gudmundsson, 2019) and tree-ring-based PDSI reconstruction (Steiger
250 et al., 2018). Lighter lines show annual values, and darker lines show 10-year moving averages.

4 Discussion

4.1 Implications of the Upper Colorado River Basin Case Study

The close agreement between reconstructed TWS anomalies and PDSI supports the overall credibility of the reconstruction
255 while also highlighting that the two records are not redundant. Although both PDSI and our TWS reconstructions use tree-

https://doi.org/10.5194/egusphere-2026-3086
Preprint. Discussion started: 12 June 2026

ring information, they are based on different chronology networks and are optimized for different hydroclimatic targets. The PDSI reconstruction of Steiger et al. (2018) uses over 80 tree-ring chronology sites for the Upper Colorado River Basin, whereas our TWS reconstruction uses only two chronologies, one of which is not included in the PDSI network (Fig. C2). Moreover, PDSI is designed to represent meteorological drought and near-surface soil moisture balance, whereas the present reconstruction targets basin-scale water storage variability. Despite their strong correlation, systematic differences are evident. For example, PDSI leads reconstructed TWS anomalies during both the onset and recovery of the 1625–1650 drought and exhibits greater variability during the 18th century (Fig. 3c). These differences are consistent with the underlying physical interpretation: PDSI primarily reflects atmospheric dryness and surface soil moisture, which respond rapidly to climate forcing, whereas TWS reflects integrated storage across soil and groundwater reservoirs, which accumulate and recover more slowly. Similar event-dependent timing differences between GRACE-derived TWS and PDSI have also been documented in the modern period (M. Zhao et al., 2017b), suggesting that these relationships reflect fundamental differences in hydrologic processes rather than artifacts of the reconstruction. Thus, the agreement between reconstructed TWS anomalies and PDSI indicates that the reconstruction captures coherent hydroclimatic variability, while the timing and amplitude differences suggest that it also provides complementary information on deeper and more integrated storage changes.

Our reconstructed TWS anomalies also agree well with climate-data-driven TWS estimates during 1901-2000, with stronger agreement in the latter half of the twentieth century and larger discrepancies earlier in the record. These early-century differences likely reflect limitations in the quality and spatial coverage of instrumental climate data used to generate the climate-data-driven estimates (Humphrey & Gudmundsson, 2019). This interpretation is supported by the consistency of the tree-ring–based TWS reconstruction with both PDSI (Fig. 3c) and previous streamflow reconstructions that indicate extraordinarily wet conditions during the 1910s (Woodhouse et al., 2006). These results suggests that tree-ring–based TWS anomaly reconstructions can provide a benchmark that is less dependent on instrumental climate data for assessing uncertainties in climate-data-driven TWS reconstructions and may also offer a useful constraint for evaluating hydrological model simulations of TWS.

4.2 Interpreting TWS-RWI correlations for TWS anomaly reconstruction

The generally modest and spatially variable correlations between TWS anomalies and RWI (Fig. 1) should be interpreted in the context of how existing tree-ring chronologies were developed. Most existing chronologies were not originally developed to represent TWS variability, but to record tree-growth responses to climatic and hydrologic factors such as temperature, precipitation, soil moisture, and streamflow. It is therefore not expected that all sites will exhibit strong correlations with TWS anomalies. As shown in Sect. 3.2, stronger correlations tend to occur in water-limited environments and among species that are more sensitive to moisture variability, whereas weaker or negative correlations are more common in energy-limited

https://doi.org/10.5194/egusphere-2026-3086
Preprint. Discussion started: 12 June 2026

settings. These patterns reflect differences in the dominant controls on tree growth, suggesting that only a subset of available chronologies may be suited for representing large-scale TWS variability.

The Upper Colorado River Basin case study shows that although only a subset of available sites exhibits strong positive TWS–RWI coupling, two chronologies are sufficient to produce a high-skill reconstruction. This demonstrates that skillful TWS reconstruction does not require uniformly strong correlations across all sites, but rather careful selection of the most informative chronologies. This perspective also suggests that sites with weak or negative correlations should not necessarily be interpreted as lacking hydrologic relevance. In the Columbia River Basin, where energy-limited conditions are more common, negative TWS–RWI correlations (Fig. 1) likely reflect snowpack impact rather than an absence of useful signal, and chronologies from such settings are frequently used in streamflow reconstruction (Littell et al., 2016, 2023). Taken together, these results suggest that chronology networks for TWS reconstruction can be designed to maximize predictive skill by spanning contrasts in snowpack influence, topographic position, groundwater contribution, rooting depth, and tree functional type, thereby capturing complementary aspects of large-scale TWS variability.

4.3 Short satellite records

A central limitation of reconstructing TWS anomalies from tree-ring records is the short duration of the GRACE observational record. This limitation is compounded by the fact that many existing tree-ring chronologies have not been updated through the GRACE era, leaving only about a decade of overlap for calibration across much of the western North America. Consequently, the statistical robustness and long-term stability of inferred TWS–RWI relationships remain limited. However, as GRACE Follow-On continues to collect observations, and with GRACE-Continuity planned for launch in 2028, the TWS anomaly satellite record will continue to lengthen, providing a progressively stronger basis for calibration and evaluation of tree-ring–based reconstructions.

To examine how record length influences the stability of TWS–RWI relationships, we used climate-data-driven TWS anomalies as a proxy for longer-term TWS variability and calculated moving correlations for each of the 144 sites using window lengths ranging from 10 to 60 years. We then quantified the stability of these relationships using the standard deviation of the moving correlations and averaged this metric across all sites (Fig. 4). The results show a clear decline in variability as the calibration window lengthens, with an apparent elbow point around 25–30 years, beyond which gains in stability become more gradual. This suggests that the current GRACE and GRACE Follow-On record is approaching the duration needed to support more stable reconstruction relationships, while also indicating that additional years of satellite observations will continue to improve reconstruction robustness.

These results point to an important opportunity for future research. Rather than waiting for a longer satellite record, now is an appropriate time to begin developing and testing tree-ring–based reconstructions of TWS anomalies, while also updating

https://doi.org/10.5194/egusphere-2026-3086
Preprint. Discussion started: 12 June 2026

existing chronologies and expanding tree-ring networks in hydrologically informative settings, including both sites with strong TWS sensitivity and contrasting environments that capture complementary controls on water storage variability. The present study lays an initial foundation for a more robust reconstruction framework. As the satellite record lengthens, this approach will become increasingly well constrained and may ultimately provide a powerful basis for extending basin-scale TWS variability beyond the satellite era, with important implications for water resources planning and hydrologic process understanding.

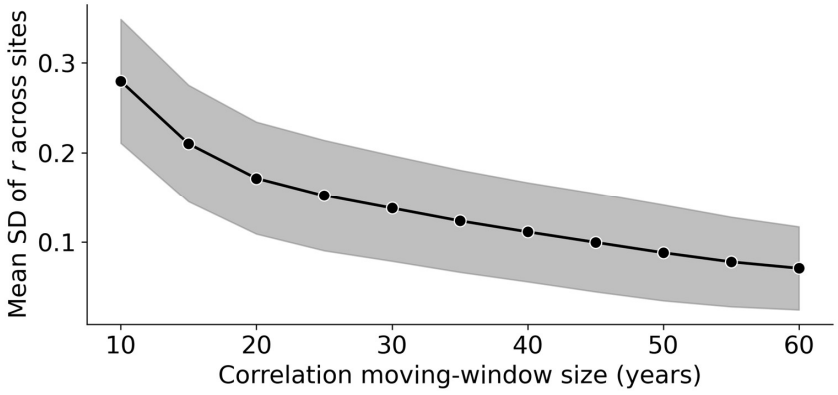

Figure 4: The current ~25-year GRACE and GRACE Follow-On record is approaching the window length needed for more stable RWI–TWS relationships. Mean standard deviation of moving correlations between RWI and climate-data-driven summer TWS anomalies across 144 sites declines with increasing window length, with gains becoming more gradual after ~25–30 years. Shading indicates ±1 standard deviation across sites. See Fig. C10 in the Supplement for maps of mean and standard deviations of correlations for windows sizes of 10, 20, 30, and 40 years

5 Conclusion

We demonstrate that moisture-sensitive tree-ring records provide a promising pathway for extending GRACE-observed TWS anomalies beyond the satellite era. Across western North America, RWI is positively correlated with GRACE-derived TWS anomalies at many sites, particularly in moisture-limited environments and during summer. The Upper Colorado River Basin case study further shows that a small number of carefully selected chronologies can capture basin-scale summer TWS variability and support reconstruction back to 1567 CE. Although the short GRACE calibration period remains an important limitation, the increasing length of the GRACE/FO record and targeted updating of tree-ring networks offer a clear path toward more robust multi-century TWS reconstructions. Such reconstructions can provide critical long-term context for interpreting recent storage changes, drought persistence, and hydroclimatic extremes, while also offering new benchmarks for evaluating climate-data-driven TWS estimates and hydrological model simulations.

https://doi.org/10.5194/egusphere-2026-3086
Preprint. Discussion started: 12 June 2026

Appendix A

We used tree-ring chronology data from Williams et al. (2020b). This dataset was selected to ensure comprehensive and comparable sites, as chronologies were processed using the state-of-the-art "signal-free" detrending method (Melvin & Briffa, 2008). The database comprises 1,498 chronologies, from which we selected 144 sites with at least 10 years of overlap with the GRACE/GRACE-FO record, as shown in Fig. C1. We follow the same site naming convention as provided in the metadata "chronology_code" column, appending the state/province acronym (from the "state_province" column) to avoid duplicate names and facilitate reference to site locations. One site, USCHUL, was listed as located in Utah (UT), but its coordinates indicate a location in Wyoming (WY); we therefore corrected the state designation for this site.

The metadata file provides a "species_code" following a four-character naming pattern. As no dictionary linking codes to species names was available, we constructed one using the fields "Species_Name", "Common_Name", and "Tree_Species_Code" from the headers of NOAA Template files "*-noaa.txt", available at https://www.ncei.noaa.gov/pub/data/paleo/treering/chronologies/northamerica/. Species names, common names, and corresponding codes for the 144 sites used in this study are listed in Table A1. Of particular note, three sites with species code "XANO" were identified as Alaska yellow cedar (*Callitropsis nootkatensis*) based on their chronology data file headers.

As described in Sect. 3.2 of the main text, tree species were grouped by genus to better characterize the influence of vegetation type on TWS–RWI correlations. For the genus *Pinus*, records were further separated by subsection to evaluate genus-level patterns. Genus assignments and *Pinus* subsections are also provided in Table A1.

The metadata from Williams et al. (2020b) lacks elevation information for several of the 144 sites used in this study, even after attempting to recover values from chronology file headers. For the 54 sites where elevation remained unavailable, missing values were filled using digital elevation model (DEM) data from the Shuttle Radar Topography Mission (SRTM), based on chronology geographic coordinates.

https://doi.org/10.5194/egusphere-2026-3086
Preprint. Discussion started: 12 June 2026

Table A1: Common names, species names, four-character species codes, genera, and subsections (for the genus *Pinus*) of the evaluated tree species.

Common name	Specie name	Code	Genera	Subsection
Alaska yellow cedar	*Callitropsis nootkatensis*	XANO	*Callitropsis*	-
Bigcone Douglas-fir	*Pseudotsuga macrocarpa (Vasey) Mayr*	PSMA	*Pseudotsuga*	-
California incense cedar	*Calocedrus decurrens (Torr.) Florin = Libocedrus decurrens Torr.*	CADE	*Calocedrus*	-
California red fir	*Abies magnifica A. Murray*	ABMA	*Abies*	-
Douglas-fir	*Pseudotsuga menziesii (Mirb.) Franco*	PSME	*Pseudotsuga*	-
Engelmann spruce	*Picea engelmannii Parry ex Engelm.*	PCEN	*Picea*	-
Foxtail pine	*Pinus balfouriana Balf.*	PIBA	*Pinus*	*P. Balfourianae*
Giant sequoia	*Sequoiadendron giganteum (Lindl.) Buchholz*	SEGI	*Sequoiadendron*	-
Intermountain bristlecone pine	*Pinus longaeva D.K. Bailey = Pinus aristata var. longaeva*	PILO	*Pinus*	*P. Balfourianae*
Jeffrey pine	*Pinus jeffreyi Balf.*	PIJE	*Pinus*	*P. Ponderosae*
Limber pine	*Pinus flexilis E. James*	PIFL	*Pinus*	*P. Strobus*
Mexican pinyon	*Pinus cembroides Zucc.*	PICM	*Pinus*	*P. Cembroides*
Mountain hemlock	*Tsuga mertensiana (Bong.) Carrière*	TSME	*Tsuga*	-
Pinyon pine	*Pinyon pine*	PIED	*Pinus*	*P. Cembroides*
Ponderosa pine	*Pinus ponderosa Douglas ex C. Lawson*	PIPO	*Pinus*	*P. Ponderosae*
Rocky Mountain juniper	*Juniperus scopulorum Sarg.*	JUSC	*Juniperus*	-
Singleleaf pinyon	*Pinus monophylla Torr. & Frém.*	PIMO	*Pinus*	*P. Cembroides*
Subalpine fir	*Abies lasiocarpa (Hook.) Nutt.*	ABLA	*Abies*	-
Subalpine larch	*Larix lyallii Parl.*	LALY	*Larix*	-
Tamarack	*Larix laricina (Du Roi) K. Koch*	LALA	*Larix*	-
Utah juniper	*Juniperus osteosperma (Torr.) Little*	JUOS	*Juniperus*	-
Western juniper	*Juniperus occidentalis Hook.*	JUOC	*Juniperus*	-

https://doi.org/10.5194/egusphere-2026-3086
Preprint. Discussion started: 12 June 2026

Appendix B

As described in Sect. 2.4 of the main text, we tested two approaches commonly used in dendrochronological reconstructions as a proof-of-concept for the Upper Colorado River Basin (UCRB), using the 11 sites located within the basin: (i) multiple linear regression (MLR), in which site predictors are added sequentially based on the Akaike information criterion (AIC), and (ii) principal component analysis (PCA). The methodology and results for each approach are described below.

Multiple Linear Regression (MLR)

For the MLR approach, we tested the progressive inclusion of sites as predictors. Sites were first ranked by their individual Pearson correlation between ring-width index (RWI) and basin-wide summer GRACE TWS over the common period (Table B1). Each subsequent site was included in the MLR model only if its addition produced a reduction in AIC; otherwise, the site was discarded and the next candidate was tested. After screening all 11 sites, only the first-ranked site (USCHUL_WY) was retained as a predictor (effectively reducing the model to a simple linear regression) as the inclusion of any additional site increased the AIC.

Table B1: Chronology sites ranked by Pearson correlation (r) between RWI and basin-wide summer GRACE/GRACE-FO TWS over the common period. The second column shows the individual site correlation computed over each chronology's full available period. AIC values in the last column correspond to the model obtained by adding each respective site to the first-ranked predictor (USCHUL_WY).

Chronology site	r	p-value	r (common period)	p-value (common period)	AIC
USCHUL_WY	0.77	0.00	0.31	0.38	97.84
JONESH_UT	0.52	0.07	0.10	0.78	99.76
NMMOAR_UT	0.48	0.11	0.00	0.99	99.83
WILDEX_CO	0.18	0.58	0.00	0.99	99.67
MAN_LW_CO	0.47	0.18	-0.03	0.94	99.23
REGNPP_UT	0.46	0.13	-0.03	0.93	99.78
UNAWEP_CO	0.76	0.00	-0.05	0.89	99.49
MAN_EW_CO	0.47	0.17	-0.07	0.84	99.21
ALMONT_CO	0.25	0.44	-0.09	0.81	99.53
MANMVR_CO	0.45	0.19	-0.10	0.78	98.98
GOULDR_CO	0.39	0.20	-0.21	0.56	99.41

https://doi.org/10.5194/egusphere-2026-3086
Preprint. Discussion started: 12 June 2026

Principial Component Analysis (PCA)

Principal component analysis (PCA) was applied to the RWI matrix of the selected chronologies over the calibration period to reduce dimensionality and extract the dominant modes of common variance. The resulting principal components (PCs) were then used as predictors in an ordinary least-squares regression against the GRACE TWS anomaly time series. Model skill was assessed using the calibration R^2, the AIC corrected for small samples (AICc), and leave-one-out cross-validation (LOO-CV) R^2 and reduction of error (RE) statistics.

All candidate models (1–3 PCs) yielded strongly negative LOO-CV R^2 and RE values, indicating that the regression failed to generalize beyond the calibration sample. Although PC1 alone explains 68.1% of the common RWI variance and shows a moderate correlation with TWS ($r = 0.60$) – see Table B2 for more details – the calibration period shared between the chronologies and GRACE/FO is too short (< 13 years) to support a stable regression, rendering the PCA-based reconstruction approach unfeasible for this basin. This result motivated the use of the mean z-score approach described in the main text.

Table B2: PCA regression calibration and validation statistics for 1–3 principal components. AICc is the AIC corrected for small samples and RE (LOO) indicates skill above the calibration mean.

PCs	Variance explained (%)	Cumulative variance (%)	R^2 (calibration)	AICc	RE (LOO)
1	68.1	68.1	0.354	67.8	−1.593
2	10.3	78.4	0.511	69.3	−1.300
3	8.2	86.6	0.567	74.1	−2.791

https://doi.org/10.5194/egusphere-2026-3086
Preprint. Discussion started: 12 June 2026

Appendix C

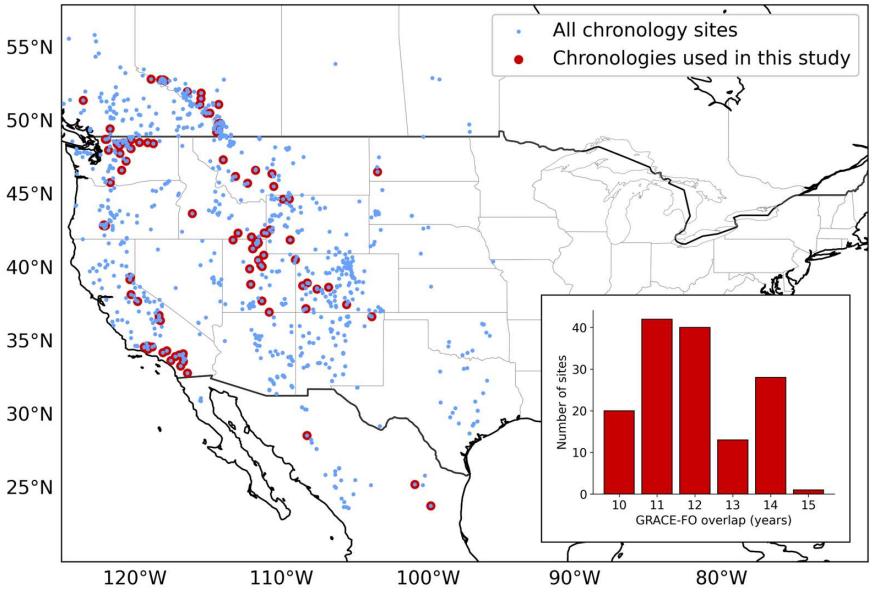

Figure C1: All tree-ring chronologies from Williams et al., 2020a are shown in blue, while the 144 sites used in this study are shown in red. The inset plot shows the total count of sites per interval of number of overlapping years for GRACE/FO period (2002-2016).

https://doi.org/10.5194/egusphere-2026-3086
Preprint. Discussion started: 12 June 2026

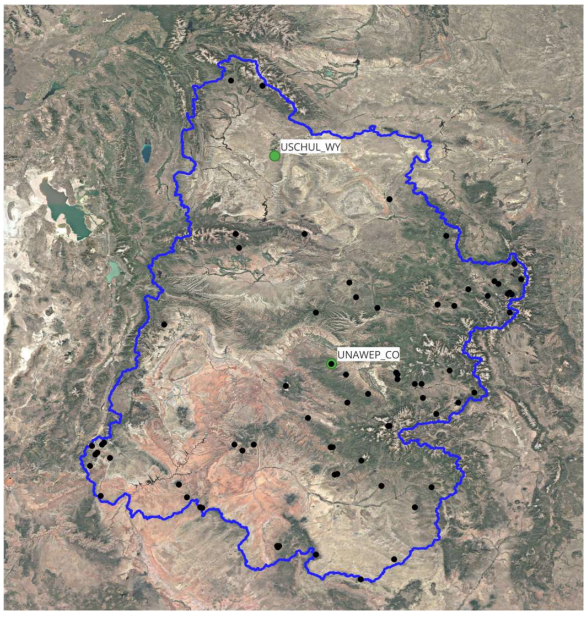

Figure C2: Location of sites USCHUL_WY and UNAWEP_CO (green markers) used in the mean z-score ring-width index for the Upper Colorado River Basin (blue boundary) summer TWS reconstruction. Black dots indicate all chronologies used for the PDSI reconstruction in Steiger et al. (2018) within the Upper Colorado River Basin. Background map imagery from Google, accessed via the Basemaps plugin in QGIS.

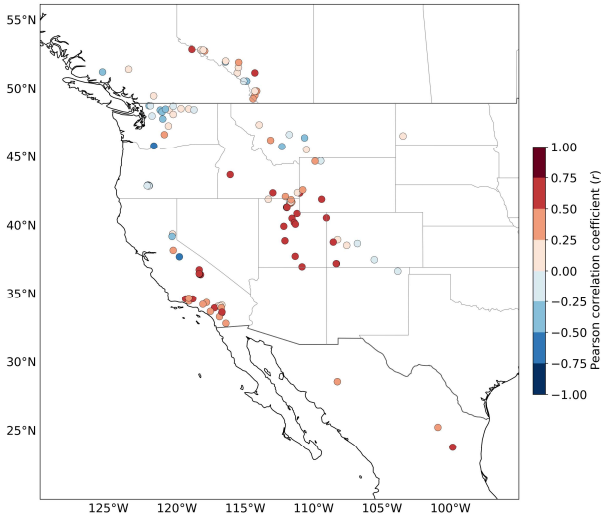

Figure C3: Pearson correlation coefficient between RWI and water-year (October to September) mean TWS.

https://doi.org/10.5194/egusphere-2026-3086
Preprint. Discussion started: 12 June 2026

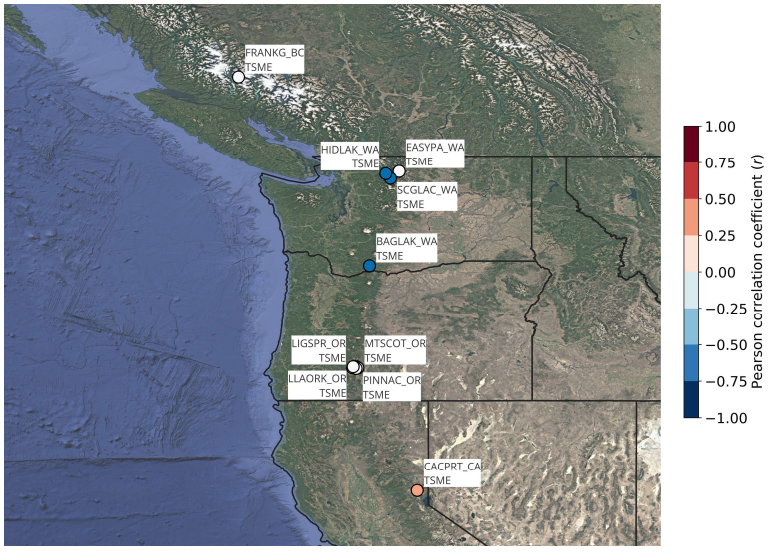

425

Figure C4: Location of sites corresponding to Mountain hemlock, Tsuga mertensiana (Bong.) Carrière (TSME). Marker colors correspond to the Pearson correlation coefficient shown in the colorbar. Background map imagery from Google, accessed via the Basemaps plugin in QGIS.

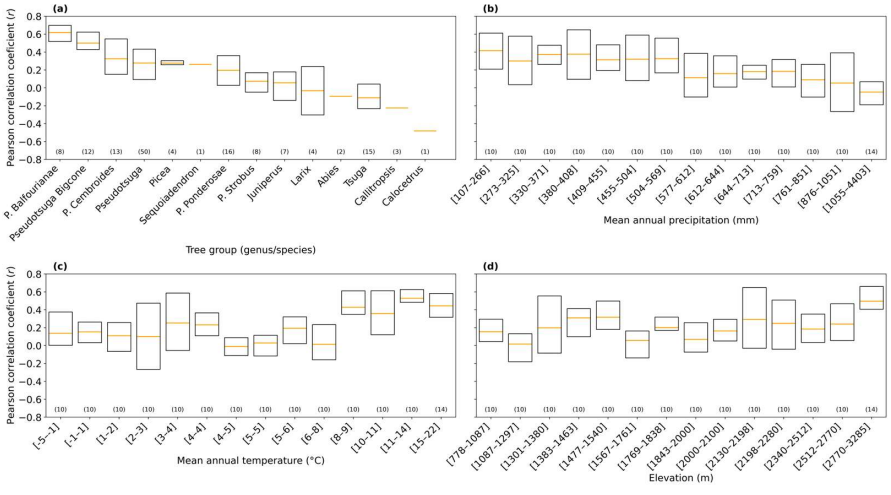

430

Figure C5: Pearson correlation coefficient distribution between spring GRACE TWS and RWI across (a) tree group (genus/subsections), (b) mean annual precipitation, (c) mean annual temperature, and (d) elevation. Boxes show the interquartile range, orange lines indicate the mean, and numbers above each bin indicate the number of sites.

https://doi.org/10.5194/egusphere-2026-3086
Preprint. Discussion started: 12 June 2026

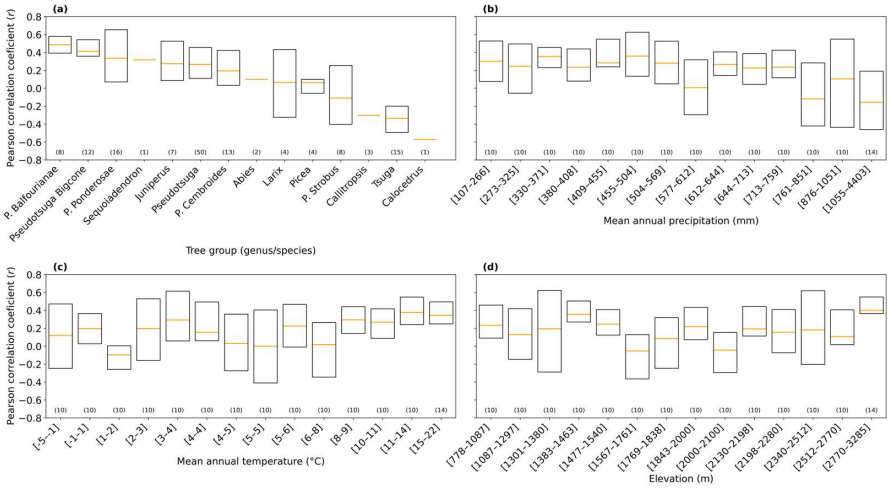

435

Figure C6: Pearson correlation coefficient distribution between fall GRACE TWS and RWI across (a) tree group (genus/subsections), (b) mean annual precipitation, (c) mean annual temperature, and (d) elevation. Boxes show the interquartile range, orange lines indicate the mean, and numbers above each bin indicate the number of sites.

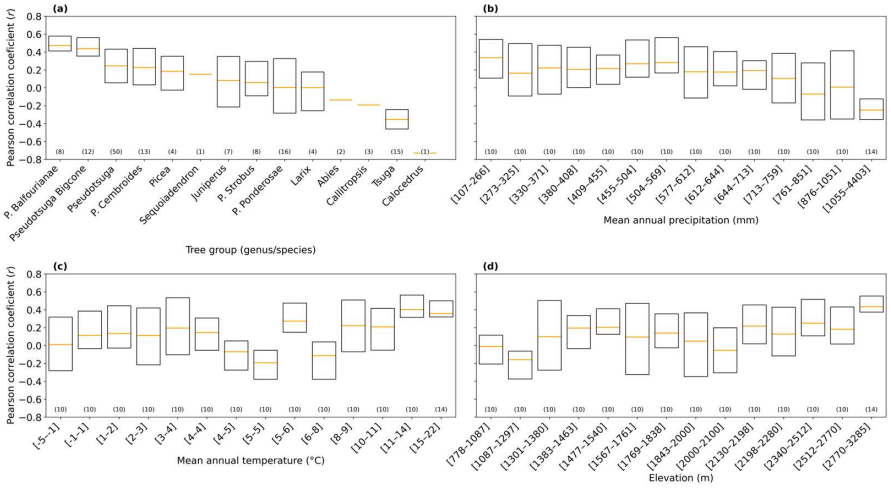

440

Figure C7: Pearson correlation coefficient distribution between winter GRACE TWS and RWI across (a) tree group (genus/subsections), (b) mean annual precipitation, (c) mean annual temperature, and (d) elevation. Boxes show the interquartile range, orange lines indicate the mean, and numbers above each bin indicate the number of sites.

https://doi.org/10.5194/egusphere-2026-3086
Preprint. Discussion started: 12 June 2026

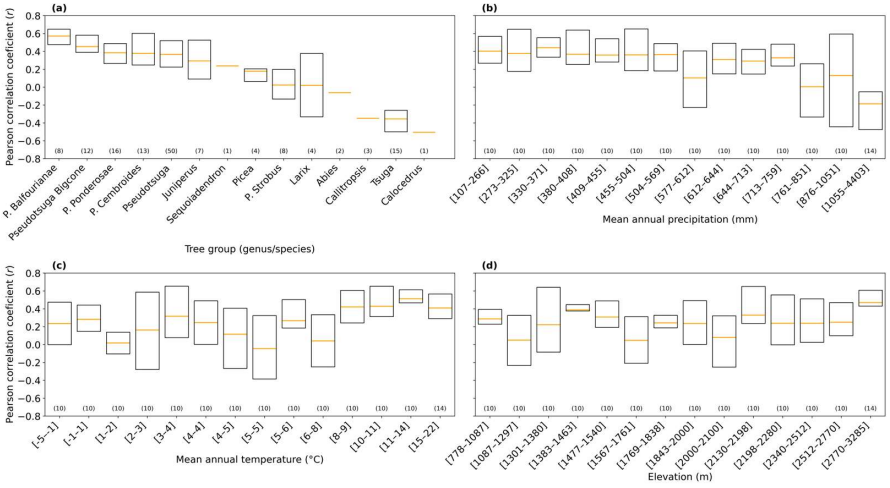

445 **Figure C8:** Pearson correlation coefficient distribution between annual (calendar year) GRACE TWS and RWI across (a) tree group (genus/subsections), (b) mean annual precipitation, (c) mean annual temperature, and (d) elevation. Boxes show the interquartile range, orange lines indicate the mean, and numbers above each bin indicate the number of sites.

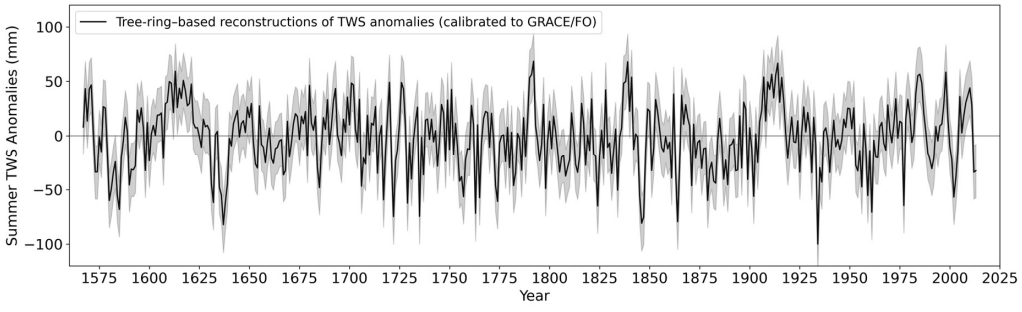

450 **Figure C9:** Ensemble mean of 1,000 Monte Carlo (MC) pseudo-simulated summer TWS reconstructions for the Upper Colorado River Basin, derived from the average RWI z-score of two tree-ring sites (USCHUL_WY and UNAWEP_CO; solid black line). Shaded envelope represents ±1 standard deviation of the 1,000 MC realizations combined with the root mean square error of the mean linear regression.

https://doi.org/10.5194/egusphere-2026-3086
Preprint. Discussion started: 12 June 2026

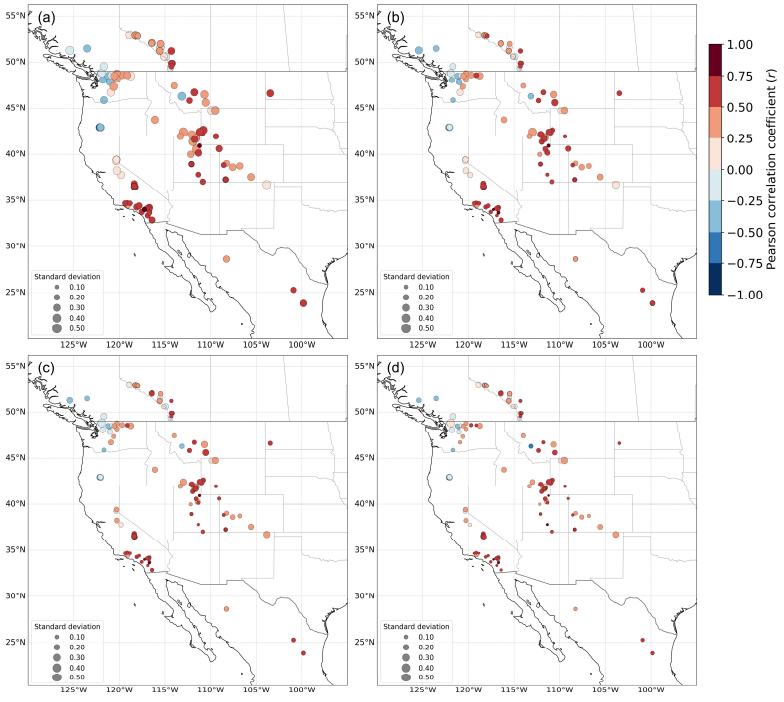

Figure C10: Mean and standard deviation of Pearson correlation coefficients from moving-window correlations between RWI and summer climate-driven TWS for window sizes of (a) 10, (b) 20, (c) 30, and (d) 40 years. Marker color indicates the mean correlation coefficient and marker size indicates its standard deviation for each site.

Data availability

Tree-ring chronologies are available at https://www.ncei.noaa.gov/access/metadata/landing-page/bin/iso?id=gov.noaa.nodc:0209529 (Williams et al., 2020b). TWS GRACE Mascon data are available at http://grace.jpl.nasa.gov (Watkins et al., 2015; Wiese et al., 2016, 2018). Climate-drive TWS reconstruction data are available at https://doi.org/10.6084/m9.figshare.7670849 (Humphrey & Gudmundsson, 2019). PDSI reconstruction data are available at https://zenodo.org/records/1198817 (Steiger, 2018).

https://doi.org/10.5194/egusphere-2026-3086
Preprint. Discussion started: 12 June 2026

Author contributions

MZ conceptualized the study. LEBH curated the data and performed the analyses. MZ and GLH contributed to the methodology. LEBH wrote the initial draft, and all authors contributed to review and editing.

Competing interests

The authors declare that they have no conflict of interest.

Acknowledgements

This study was funded by NASA grant 80NSSC24M0114 and NSF grant 2429739 awarded to the University of Idaho.

References

Buzzanga, B., Hamlington, B., Fasullo, J., Landerer, F., & Peidou, A. (2025). Interdecadal variability of terrestrial water storage since 2003. Communications Earth & Environment, 6(1), 246.

Chandanpurkar, H. A., Famiglietti, J. S., Gopalan, K., Wiese, D. N., Wada, Y., Kakinuma, K., et al. (2025). Unprecedented continental drying, shrinking freshwater availability, and increasing land contributions to sea level rise. Science Advances, 11(30), eadx0298. https://doi.org/10.1126/sciadv.adx0298

Cook, E. R., & Peters, K. (1997). Calculating unbiased tree-ring indices for the study of climatic and environmental change. The Holocene, 7(3), 361–370.

Cook, E. R., Woodhouse, C. A., Eakin, C. M., Meko, D. M., & Stahle, D. W. (2004). Long-term aridity changes in the western United States. Science, 306(5698), 1015–1018.

Cook, E. R., Seager, R., Heim Jr, R. R., Vose, R. S., Herweijer, C., & Woodhouse, C. (2010). Megadroughts in North America: placing IPCC projections of hydroclimatic change in a long-term palaeoclimate context. Journal of Quaternary Science, 25(1), 48–61. https://doi.org/10.1002/jqs.1303

Creutzfeldt, B., Heinrich, I., & Merz, B. (2015). Total water storage dynamics derived from tree-ring records and terrestrial gravity observations. Advances in Paleohydrology Research and Applications, 529, 640–649. https://doi.org/10.1016/j.jhydrol.2015.04.006

Fritts, H. C. (2012). Tree rings and climate. Elsevier.

Fritts, H. C., Mosimann, J. E., & Bottorff, C. P. (1969). A revised computer program for standardizing tree-ring series.

Gedalof, Z., & Smith, D. J. (2001). Interdecadal climate variability and regime-scale shifts in Pacific North America. Geophysical Research Letters, 28(8), 1515–1518. https://doi.org/10.1029/2000GL011779

https://doi.org/10.5194/egusphere-2026-3086
Preprint. Discussion started: 12 June 2026

Hacker, C., Gutknecht, B. D., Löcher, A., & Kusche, J. (2026). Multidecadal reconstruction of terrestrial water storage changes by combining pre-GRACE satellite observations and climate data. Earth System Science Data, 18(3), 1747–1781. https://doi.org/10.5194/essd-18-1747-2026

Hoaglin, D. C., Mosteller, F., & Tukey, J. W. (2000). Understanding robust and exploratory data analysis. John Wiley & Sons.

Humphrey, V., & Gudmundsson, L. (2019). GRACE-REC: a reconstruction of climate-driven water storage changes over the last century. Earth System Science Data, 11(3), 1153–1170. https://doi.org/10.5194/essd-11-1153-2019

Li, F., Kusche, J., Rietbroek, R., Wang, Z., Forootan, E., Schulze, K., & Lück, C. (2020). Comparison of Data-Driven Techniques to Reconstruct (1992–2002) and Predict (2017–2018) GRACE-Like Gridded Total Water Storage Changes Using Climate Inputs. Water Resources Research, 56(5), e2019WR026551. https://doi.org/https://doi.org/10.1029/2019WR026551

Li, F., Kusche, J., Chao, N., Wang, Z., & Löcher, A. (2021). Long-Term (1979-Present) Total Water Storage Anomalies Over the Global Land Derived by Reconstructing GRACE Data. Geophysical Research Letters, 48(8), e2021GL093492. https://doi.org/https://doi.org/10.1029/2021GL093492

Littell, J. S., Pederson, G. T., Gray, S. T., Tjoelker, M., Hamlet, A. F., & Woodhouse, C. A. (2016). Reconstructions of Columbia River Streamflow from Tree-Ring Chronologies in the Pacific Northwest, USA. JAWRA Journal of the American Water Resources Association, 52(5), 1121–1141. https://doi.org/10.1111/1752-1688.12442

Littell, J. S., Pederson, G. T., Martin, J. T., & Gray, S. T. (2023). Networks of Tree-Ring Based Streamflow Reconstructions for the Pacific Northwest, U.S.A. Water Resources Research, 59(11), e2023WR035255. https://doi.org/10.1029/2023WR035255

Maxwell, J. T., Harley, G. L., Tucker, C. S., Galuska, T., Ficklin, D. L., Bregy, J. C., et al. (2022). 1,100-Year Reconstruction of Baseflow for the Santee River, South Carolina, USA Reveals Connection to the North Atlantic Subtropical High. Geophysical Research Letters, 49(22), e2022GL100742. https://doi.org/10.1029/2022GL100742

McCormick, E. L., Dralle, D. N., Hahm, W. J., Tune, A. K., Schmidt, L. M., Chadwick, K. D., & Rempe, D. M. (2021). Widespread woody plant use of water stored in bedrock. Nature, 597(7875), 225–229. https://doi.org/10.1038/s41586-021-03761-3

Meko, D., & Woodhouse, C. (2010). Application of streamflow reconstruction to water resources management. In Dendroclimatology: Progress and prospects (pp. 231–261). Springer.

Meko, D., Cook, E. R., Stahle, D. W., Stockton, C. W., & Hughes, M. K. (1993). Spatial patterns of tree-growth anomalies in the United States and southeastern Canada. Journal of Climate, 6(9), 1773–1786.

Melvin, T. M., & Briffa, K. R. (2008). A “signal-free” approach to dendroclimatic standardisation. Dendrochronologia, 26(2), 71–86. https://doi.org/https://doi.org/10.1016/j.dendro.2007.12.001

Melvin, T. M., Briffa, K. R., Nicolussi, K., & Grabner, M. (2007). Time-varying-response smoothing. Dendrochronologia, 25(1), 65–69.

https://doi.org/10.5194/egusphere-2026-3086
Preprint. Discussion started: 12 June 2026

NASA. (2013). Shuttle Radar Topography Mission (SRTM) Global. Distributed by OpenTopography. Accessed 2026-03-13. [Data set]. https://doi.org/https://doi.org/10.5069/G9445JDF

Rasmussen, R. M., Chen, F., Liu, C., Ikeda, K., Prein, A., Kim, J., et al. (2023). CONUS404: Four-kilometer long-term regional hydroclimate reanalysis over the conterminous United States (ver. 2.0, December 2023). U.S. Geological Survey. https://doi.org/10.5066/P9PHPK4F

Reager, J. T., Thomas, B. F., & Famiglietti, J. S. (2014). River basin flood potential inferred using GRACE gravity observations at several months lead time. Nature Geoscience, 7(8), 588–592. https://doi.org/10.1038/ngeo2203

Rodell, M., & Li, B. (2023). Changing intensity of hydroclimatic extreme events revealed by GRACE and GRACE-FO. Nature Water, 1(3), 241–248. https://doi.org/10.1038/s44221-023-00040-5

Rodell, M., Famiglietti, J. S., Wiese, D. N., Reager, J. T., Beaudoing, H. K., Landerer, F. W., & Lo, M.-H. (2018). Emerging trends in global freshwater availability. Nature, 557(7707), 651–659. https://doi.org/10.1038/s41586-018-0123-1

Singh Chuphal, D., Thirumalai, K., & Mishra, V. (2025). Recent drying of the Ganga River is unprecedented in the last 1,300 years. Proceedings of the National Academy of Sciences, 122(40), e2424613122.

Speer, J. H. (2010). Fundamentals of tree-ring research. University of Arizona Press.

Steiger, N. J. (2018). Paleo Hydrodynamics Data Assimilation product (PHYDA) [Data set]. Zenodo. https://doi.org/10.5281/zenodo.1198817

Steiger, N. J., Smerdon, J. E., Cook, E. R., & Cook, B. I. (2018). A reconstruction of global hydroclimate and dynamical variables over the Common Era. Scientific Data, 5(1), 180086. https://doi.org/https://doi.org/10.1038/sdata.2018.86

Stocker, B. D., Tumber-Dávila, S. J., Konings, A. G., Anderson, M. C., Hain, C., & Jackson, R. B. (2023). Global patterns of water storage in the rooting zones of vegetation. Nature Geoscience, 16(3), 250–256. https://doi.org/10.1038/s41561-023-01125-2

Tapley, B. D., Bettadpur, S., Ries, J. C., Thompson, P. F., & Watkins, M. M. (2004). GRACE measurements of mass variability in the Earth system. Science, 305(5683), 503–505.

Thomas, A. C., Reager, J. T., Famiglietti, J. S., & Rodell, M. (2014). A GRACE-based water storage deficit approach for hydrological drought characterization. Geophysical Research Letters, 41(5), 1537–1545. https://doi.org/10.1002/2014GL059323

Watkins, M. M., Wiese, D. N., Yuan, D.-N., Boening, C., & Landerer, F. W. (2015). Improved methods for observing Earth's time variable mass distribution with GRACE using spherical cap mascons. Journal of Geophysical Research: Solid Earth, 120(4), 2648–2671. https://doi.org/https://doi.org/10.1002/2014JB011547

Wiese, D. N., Landerer, F. W., & Watkins, M. M. (2016). Quantifying and reducing leakage errors in the JPL RL05M GRACE mascon solution. Water Resources Research, 52(9), 7490–7502. https://doi.org/https://doi.org/10.1002/2016WR019344

Wiese, D. N., Yuan, D.-N., Boening, C., Landerer, F. W., & Watkins, M. M. 2018. (2018). JPL GRACE Mascon Ocean, Ice, and Hydrology Equivalent Water Height Release 06 Coastal Resolution Improvement (CRI) Filtered Version 1.0. Dataset

https://doi.org/10.5194/egusphere-2026-3086
Preprint. Discussion started: 12 June 2026

accessed [2026-01-23] at https://doi.org/10.5067/TEMSC-3MJC6. NASA Physical Oceanography Distributed Active Archive Center. https://doi.org/10.5067/TEMSC-3MJC6

Williams, A. P., Cook, E. R., Smerdon, J. E., Cook, B. I., Abatzoglou, J. T., Bolles, K., et al. (2020a). Large contribution from anthropogenic warming to an emerging North American megadrought. Science, 368(6488), 314–318. https://doi.org/10.1126/science.aaz9600

Williams, A. P., Cook, E. R., Smerdon, J. E., Cook, B. I., Abatzoglou, J. T., Bolles, K., et al. (2020b). Large contribution from anthropogenic warming to an emerging North American megadrought (NCEI Accession 0209529). Subset ./2.2/data/0-data/megadrought/rwi_data/. NOAA National Centers for Environmental Information. https://doi.org/https://doi.org/10.25921/2vbe-8092.

Williams, A. P., Cook, B. I., & Smerdon, J. E. (2022). Rapid intensification of the emerging southwestern North American megadrought in 2020–2021. Nature Climate Change, 12(3), 232–234. https://doi.org/10.1038/s41558-022-01290-z

Woodhouse, C. A. (2003). A 431-yr reconstruction of western Colorado snowpack from tree rings. Journal of Climate, 16(10), 1551–1561.

Woodhouse, C. A., Gray, S. T., & Meko, D. M. (2006). Updated streamflow reconstructions for the Upper Colorado River Basin. Water Resources Research, 42(5). https://doi.org/10.1029/2005WR004455

Yang, B., Qin, C., Wang, J., He, M., Melvin, T. M., Osborn, T. J., & Briffa, K. R. (2014). A 3,500-year tree-ring record of annual precipitation on the northeastern Tibetan Plateau. Proceedings of the National Academy of Sciences, 111(8), 2903–2908. https://doi.org/10.1073/pnas.1319238111

Yin, J., Slater, L. J., Khouakhi, A., Yu, L., Liu, P., Li, F., et al. (2023). GTWS-MLrec: global terrestrial water storage reconstruction by machine learning from 1940 to present. Earth System Science Data, 15(12), 5597–5615. https://doi.org/10.5194/essd-15-5597-2023

Zhao, M., A, G., Velicogna, I., & Kimball, J. S. (2017a). A Global Gridded Dataset of GRACE Drought Severity Index for 2002–14: Comparison with PDSI and SPEI and a Case Study of the Australia Millennium Drought. Journal of Hydrometeorology, 18(8), 2117–2129. https://doi.org/10.1175/JHM-D-16-0182.1

Zhao, M., A, G., Velicogna, I., & Kimball, J. S. (2017b). Satellite observations of regional drought severity in the continental United States using GRACE-based terrestrial water storage changes. Journal of Climate, 30(16), 6297–6308.

Zhao, M., A, G., Zhang, J., Velicogna, I., Liang, C., & Li, Z. (2021). Ecological restoration impact on total terrestrial water storage. Nature Sustainability, 4(1), 56–62.

Zhao, M., McCormick, E. L., A, G., Konings, A. G., & Li, B. (2025). Substantial root-zone water storage capacity observed by GRACE and GRACE/FO. Hydrol. Earth Syst. Sci., 29(10), 2293–2307. https://doi.org/10.5194/hess-29-2293-2025

Zhao, Y., Hoeltgebaum, L. E. B., Kukal, M. S., & Zhao, M. (2025). Leading satellite-based evapotranspiration products insufficiently capture interannual variability: Evidence from GRACE/FO and in situ observations. Geophysical Research Letters, 52(19), e2025GL116784.